REPORT DOCUMENTATION PAGE

Form Approved
OMB No. 0704-0188

1. REPORT DATE *(DD-MM-YYYY)*	2. REPORT TYPE	3. DATES COVERED *(From - To)*
04-02-2008	Conference Proceeding	

4. TITLE AND SUBTITLE
Determination of Primary Bands for Global Ocean-color Remote Sensing

5a. CONTRACT NUMBER

5b. GRANT NUMBER

5c. PROGRAM ELEMENT NUMBER
0602435N

6. AUTHOR(S)
Zhongping Lee, Robert A. Arnone, K. L. Carder, MingXia He

5d. PROJECT NUMBER

5e. TASK NUMBER

5f. WORK UNIT NUMBER
73-6734-A7-5

7. PERFORMING ORGANIZATION NAME(S) AND ADDRESS(ES)
Naval Research Laboratory
Oceanography Division
Stennis Space Center, MS 39529-5004

8. PERFORMING ORGANIZATION REPORT NUMBER
NRL/PP/7330-07-7247

9. SPONSORING/MONITORING AGENCY NAME(S) AND ADDRESS(ES)
Office of Naval Research
800 N. Quincy St.
Arlington, VA 22217-5660

10. SPONSOR/MONITOR'S ACRONYM(S)
ONR

11. SPONSOR/MONITOR'S REPORT NUMBER(S)

12. DISTRIBUTION/AVAILABILITY STATEMENT
Approved for public release, distribution is unlimited.

13. SUPPLEMENTARY NOTES

14. ABSTRACT

A few years ago, Lee and Carder demonstrated that for the quantitative derivation of major properties in an aqua-environment (information of phytoplankton biomass, colored dissolved organic matter, and bottom status) from remote sensing of its color, a sensor with roughly ~17 spectral bands in the 400 • 800 nm range can provide acceptable results compared to a sensor with 81 consecutive bands (in a 5-nm step). In that study, however, it did not show where the 17 bands should be placed. Here, from nearly 300 hyperspectral measurements of water reflectance taken in both coastal and oceanic waters that covering both optically deep and optically shallow waters, first and second derivatives were calculated after interpolating the measurements into 1-nm resolution. From these hyperspectral derivatives, the occurrence of zero value at each wavelength was accounted for, and a spectrum of the total occurrences was obtained, and further the wavelengths that captured most number of zeros were identified. Because these spectral locations indicate extremum (a local maximum or minimum) of the reflectance spectrum or inflections of the spectral curvature, placing the bands of a sensor at these wavelengths maximize the possibility of capturing (and then accurately restoring) the detailed curve of a reflectance spectrum, and thus maximize the potential of detecting the changes of water and/or bottom properties of various aqua environments with a multi-band sensor.

15. SUBJECT TERMS
ocean color remote sensing, spectral bands

16. SECURITY CLASSIFICATION OF:			17. LIMITATION OF ABSTRACT	18. NUMBER OF PAGES	19a. NAME OF RESPONSIBLE PERSON
a. REPORT	b. ABSTRACT	c. THIS PAGE			Zhongping Lee
Unclassified	Unclassified	Unclassified	UL	7	19b. TELEPHONE NUMBER *(Include area code)* 228-688-4873

Determination of primary bands for global ocean-color remote sensing

ZhongPing Lee[1], Robert Arnone[1], Kendall Carder[2], MingXia He[3]

[1] Naval Research Lab, Code 7330, Stennis Space Center, MS 39529, USA
[2] College of Marine Science, St. Petersburg, FL 33701, USA
[3] Ocean Remote Sensing Institute, Ocean University of China, Qingdao, China

ABSTRACT

A few years ago, Lee and Carder[1] demonstrated that for the quantitative derivation of major properties in an aqua-environment (information of phytoplankton biomass, colored dissolved organic matter, and bottom status, for instance) from remote sensing of its color, a sensor with roughly ~17 spectral bands in the 400 – 800 nm range can provide acceptable results compared to a sensor with 81 consecutive bands (in a 5-nm step). In that study, however, it did not show where the 17 bands should be placed. Here, from nearly 300 hyperspectral measurements of water reflectance taken in both coastal and oceanic waters that covering both optically deep and optically shallow waters, first and second derivatives were calculated after interpolating the measurements into 1-nm resolution. From these hyperspectral derivatives, the occurrence of zero value at each wavelength was accounted for, and a spectrum of the total occurrences was obtained, and further the wavelengths that captured most number of zeros were identified. Because these spectral locations indicate extremum (a local maximum or minimum) of the reflectance spectrum or inflections of the spectral curvature, placing the bands of a sensor at these wavelengths maximize the possibility of capturing (and then accurately restoring) the detailed curve of a reflectance spectrum, and thus maximize the potential of detecting the changes of water and/or bottom properties of various aqua environments with a multi-band sensor.

Keywords: Ocean-color remote sensing, spectral bands

1. INTRODUCTION

Since the successful demonstration of the Coastal Zone Color Scanner (CZCS) in measuring the spatial and temporal variation of ocean color[2, 3], the importance of observing ocean and coastal waters with sensors in the visible domain is getting more and more attention from various countries. Especially, after the launch of the SeaWiFS and MODIS satellites about ten years ago and the successful and exceptional results of such data since then, more and more satellite sensors have been (or planned to be) launched for the observation of global ocean via observing the water color. These include the COCTS of China, the MERIS of ESA, the OCM of India, and the GOCI of Korea[4], etc.

Ideally, to maximize the potential of observing properties of aqua-environment and their temporal and spatial changes, it is best to have a sensor capable of colleting signals with a continuous spectrum. After consideration of data flow, processing, and storage as well as signal-to-noise ratio, satellite sensors commonly have a few bands in the visible domain[4]. For instance, the CZCS had five bands, while SeaWiFS and MODIS have six bands (with slightly different configurations). Selection of those bands (number of bands and their center wavelengths as well as band widths) was based on the optical characteristics (both absorption and scattering) of phytoplankton and colored dissolved organic matter[4]. Thus these configurations

Coastal Ocean Remote Sensing, edited by Robert J. Frouin, ZhongPing Lee,
Proc. of SPIE Vol. 6680, 66800D, (2007) · 0277-786X/07/$18 · doi: 10.1117/12.731940

are in general good for monitoring chlorophyll concentrations (index of phytoplankton) and CDOM in the open oceans, but not optimal for remote-sensing of complex coastal waters. Lee and Carder[1] demonstrated that for adequate remote sensing of major properties (water column and bottom) of both open ocean and complex coastal aqua-environments, a sensor requires ~ 17 spectral bands in the 400 – 800 nm range to obtain similar results as a sensor with 81 consecutive bands in a 5-nm spacing. It is not yet clear, however, where the 17 bands should be placed.

In this study, with an aim for future advanced sensor for observing properties of most aqua-environments from water color, we derived the spectral locations of the optimal bands through first- and second derivatives of the remote sensing reflectance. These bands thus can capture most of the spectral variations of remote-sensing reflectance caused by varying water column and/or bottom properties.

2. DATA AND METHOD

Since 1993, in a life span of more than 12 years, an extensive data set of hyperspectral (~350 – 900 nm with a resolution ~2 nm) remote-sensing reflectance for various types of water was collected, with most of them measured by the group lead by Prof. Kendall Carder at the College of Marine Science of the University of South Florida. Table 1 summarizes the cruises and general information of the various environments. The measured waters included open ocean blue waters to turbid coastal yellowish waters and optically shallow waters. Wide ranges of concentrations of chlorophyll and dissolved organic matter and suspended sediments, along with different types of phytoplankton taxonomy were encountered.

Table 1: Data used in this study (a total of 298 stations)

AREA	DATE	# OF STATIONS	[CHL] RANGE
Gulf of Mexico	Apr 1993	24	0.07 – 49.0
Florida Keys	July 1994	5	0.06 – 0.5
Arabian Sea	Dec 1994	20	0.3 – 0.9
Chesapeake Bay	Sept 1996	36	1.7 – 20.7
Hawaii	Feb 1997	6	0.1 – 0.3
Florida Keys	May 1997	8	N/A
East China Sea	July 1998	37	0.5 – 2.8
California Coast	Oct 1999	37	0.2 – 9.4
North Atlantic	July 2001	17	4.5 – 13.9
Monterey Bay	Apr 2003	56	0.1 – 9.7
Ft. Lauderdale	July 2005	52	N/A

Remote-sensing reflectance ($R_{rs}(\lambda)$) is defined as the ratio of water-leaving radiance to downwelling irradiance. For each station of the many cruises, using a handheld spectroradiometer (Spectron Model SE-590 of Spectron Engineering before 1997; SPECTRIX for 1997 and later), a series (~ 3 to 5 scans) of upwelling radiance above the surface ($L_u(0^+)$) and the downwelling sky radiance (L_{sky}) were directly measured by the instruments. The measured L_u is a sum of photons emerged from subsurface scattering (the desired signal) plus surface reflected sky and solar light (noise). Downwelling irradiance was derived by measuring the radiance (L_R) reflected from a standard diffuse reflector (Spectralon®). For each of the collected scans, hyperspectral total-remote-sensing reflectance ($T_{rs}(\lambda)$) and sky reflectance ($S_{rs}(\lambda)$) were derived through

$$T_{rs} = \frac{L_u}{L_R}\frac{R_R}{\pi} \quad \text{and} \quad S_{rs} = \frac{L_{sky}}{L_R}\frac{R_R}{\pi}, \tag{1}$$

with R_R the reflectance of the diffuse reflector (~ 10%).

Based on these measured T_{rs} and S_{rs} curves, averages of T_{rs} and S_{rs} for each station were obtained, respectively, in order to reduce the random variations associated with measurements due to reflection from different wave facets, etc. Further, because T_{rs} is the sum of water-leaving radiance and radiance reflected by the water surface, $R_{rs}(\lambda)$ is calculated as[5, 6]

$$R_{rs}(\lambda) = T_{rs}(\lambda) - F\,S_{rs}(\lambda) - \Delta, \tag{2}$$

where F is surface Fresnel reflectance (around 0.023 for the viewing geometry), and Δ accounts for the residual surface contribution (glint, etc.). Figure 1 shows some examples of spectral T_{rs} and S_{rs}, while Figure 2 shows examples of $R_{rs}(\lambda)$. Clearly, as already well known, S_{rs} spectra are monotonic decreasing functions of λ, where as T_{rs} spectra, because of the contribution of R_{rs}, show distinct variations from water to water.

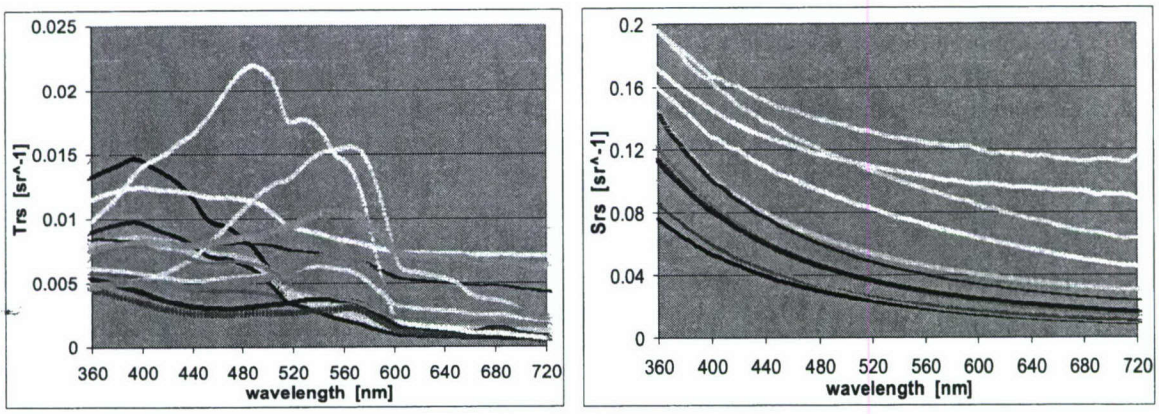

Fig. 1. Examples of T_{rs} and S_{rs} spectra used in this study.

R_{rs} is a function of the total absorption and backscattering coefficients[7-10]. Spectra of backscattering coefficients, although normally stronger in the shorter wavelengths, generally do not have strong spectral signatures[3, 11]. The spectrum of total absorption coefficient, however, is an additive result from the contributions of CDOM, various pigments contained in phytoplankton, plus water molecules[3, 12]. These contributions are spectrally selective, thus resulted significant variations in the spectral signatures of total absorption coefficient[13, 14]. The extremum values (local maximum or minimum) of $R_{rs}(\lambda)$ and the inflections of $R_{rs}(\lambda)$ indicate the different combinations of those optically active constituents and/or bottom properties. If a sensor has only a few spectral bands, to best capture the spectral signatures of $R_{rs}(\lambda)$, then these bands need to be positioned at wavelengths that can match the locations of those extremums and inflections of $R_{rs}(\lambda)$. The spectral locations of the extremums and inflections of $R_{rs}(\lambda)$ are those wavelengths with zero

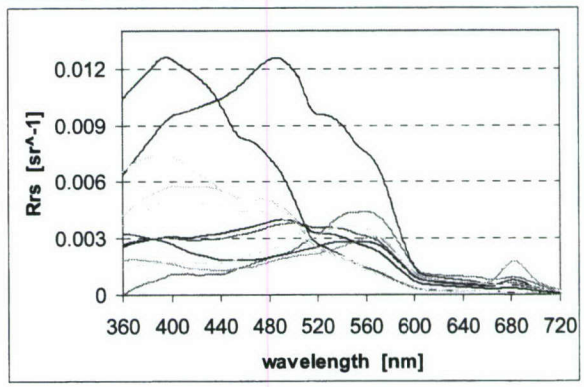

Fig. 2. Examples of $R_{rs}(\lambda)$ used in this study.

first- and second-order derivatives of $R_{rs}(\lambda)$, respectively.

To find out the optimal spectral locations for all collected samples, we carried out the following calculations:

$$\sigma(\lambda) = \frac{d R_{rs}(\lambda)}{d\lambda}$$
$$\varsigma(\lambda) = \frac{d \sigma(\lambda)}{d\lambda} \quad , \tag{3}$$

where $\sigma(\lambda)$ and $\varsigma(\lambda)$ are the first- and second-order derivatives of $R_{rs}(\lambda)$, respectively. Before calculating the derivatives, $R_{rs}(\lambda)$ spectrum was interpolated into 1-nm resolution and was smoothed with a 5-nm running average (to remove some of the random noises). Figure 3 presents examples of $\sigma(\lambda)$ and $\varsigma(\lambda)$ of the data set.

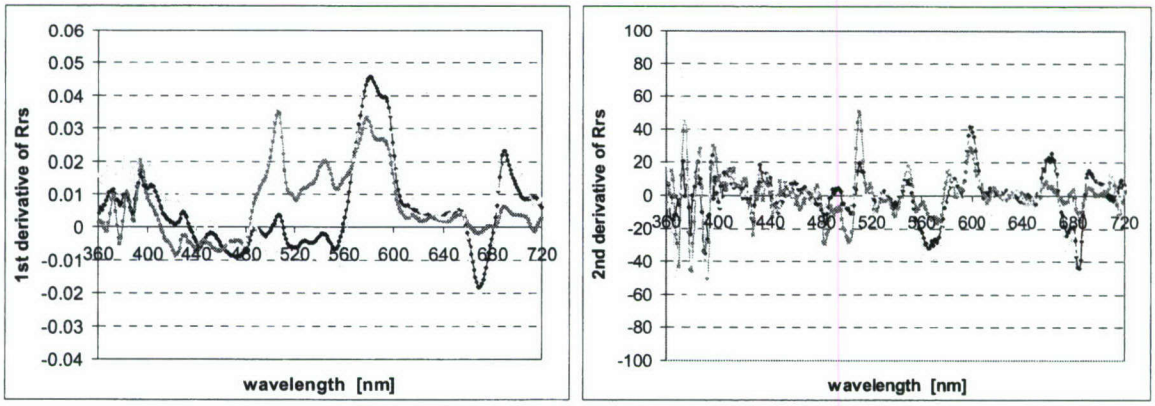

Fig. 3. Examples of $\sigma(\lambda)$x10000 (Left) and $\varsigma(\lambda)$x1000 (Right).

3. RESULTS AND DISCUSSION

From all of the calculated $\sigma(\lambda)$ and $\varsigma(\lambda)$ spectra, we obtained the spectral distribution (in 1-nm resolution) where $\sigma(\lambda)$ and $\varsigma(\lambda)$ equal zero, respectively. Mathematically, these distributions are,

$$f_\sigma(\lambda) = \frac{\sum_{i=1}^{N} \sigma_i(\lambda) = 0}{N},$$
$$f_\varsigma(\lambda) = \frac{\sum_{i=1}^{N} \varsigma_i(\lambda) = 0}{N}. \tag{4}$$

Here $\sigma_i(\lambda)$ and $\varsigma_i(\lambda)$ are the ith $\sigma(\lambda)$ and $\varsigma(\lambda)$ spectrum, respectively. Figure 4 shows $f_\sigma(\lambda)$ and $f_\varsigma(\lambda)$ (after a 5-nm running average to highlight the major bands) of this study.

For an $R_{rs}(\lambda)$ spectrum, $\sigma(\lambda) = 0$ indicates that there is an extremum R_{rs} value at λ. For various waters, because of the different combinations of water constituents and/or bottom characteristics, the locations of the extremums shifts (see Fig.2). The spectral distribution of $f_\sigma(\lambda)$ then summaries, for all data in this study, the wavelength behavior in capturing the extremums. The greater the $f_\sigma(\lambda)$ value, the more the appearance of an

extremum at that λ. Apparently, from this extensive data set, the bands that captured more extremums of R_{rs} are concentrated to seven bands (in the 360 – 700 nm range) instead of scattered to all bands (see Fig.4, Left). The seven bands are centered at (round to nearest 0 or 5): 395, 440, 490, 515, 565, 665, and 685 nm. Such a result is not surprising. For instance, 440 nm is at the peak absorption of phytoplankton pigments (chlorophyll-a), which normally causes a local minimum of $R_{rs}(\lambda)$; on the other hand, 685 nm is around the peak of chlorophyll fluorescence, which normally contributes a local maximum of $R_{rs}(\lambda)$ (see Fig.2). This result from the analysis of the first derivative is consistent with the results of the principal component analysis[15] where five bands in the 400 – 600 nm range were suggested for the detection of phytoplankton. Therefore, for a multi-band sensor, it requires that it has at least these bands to best capture the extremums of the various $R_{rs}(\lambda)$ spectra.

$\varsigma(\lambda) = 0$, on the other hand, indicates an inflection of an $R_{rs}(\lambda)$ curvature at λ, normally resulted from different combinations of pigments and water molecules, and/or bottom effects. Table 2 summarizes the wavelengths that capture more inflections of $R_{rs}(\lambda)$ curves (see Fig. 4, Right). Different from the distribution of $f_\sigma(\lambda)$, the greater values of $f_\varsigma(\lambda)$ are much less concentrated spectrally. Such a result, however, does indicate that our data set covers a wide range of water environments, which encompass various types of phytoplankton classes (resulted minor changes in $R_{rs}(\lambda)$ curvatures because of pigment absorption). For a multi-band sensor, it is necessary to have bands cover these wavelengths if pigment compositions (related to phytoplankton classes and/or functional groups) and/or bottom properties are also desired from remote sensing of water color. Interestingly, these bands match very well with the center wavelengths of the major pigments (Table 2) of presented in Hoepffner and Sathyendranath[16].

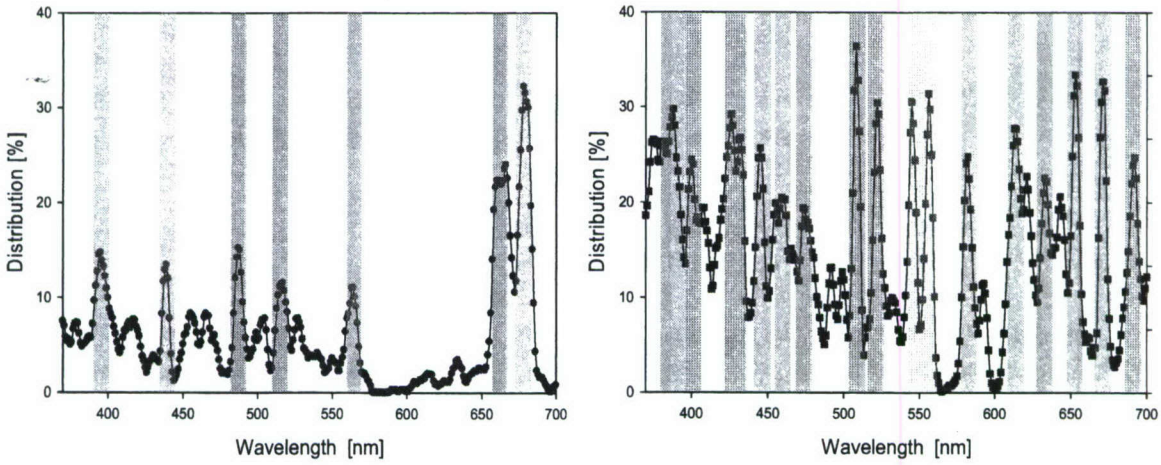

Fig. 4. Distributions of $f_\sigma(\lambda)$ (Left) and $f_\varsigma(\lambda)$ (Right).

Consolidating the major bands that have greater values of $f_\sigma(\lambda)$ and $f_\varsigma(\lambda)$ (and considering a 10-20 nm bandwidth for satellite sensors), possible bands for future sensors are suggested (Table 2), although absorption effects by gases in the atmosphere are not considered yet. Interestingly, the analysis from the first- and second-order derivative also indicates a number of 16 bands for the observation of ocean color. We added a band at 710 nm, consistent with the configuration of MERIS, although not a big number of $f_\sigma(710)$ was obtained (because of low number of observations of such extreme cases). This band, however, is important for turbid coastal water and water with extreme phytoplankton blooms (red tide)[17, 18].

Table 2 also presents, as an example, the spectral bands of MODIS and MERIS. Clearly, the wavelengths of those bands are in general consistent with findings presented here. Comparing MODIS bands with that from this study and that of MERIS, the significant shortage of MODIS (and SeaWiFS) is a band between 551 and 667 nm. Such a band is of great value for remote sensing of suspended sediments[19] or remote sensing of optically shallow waters.

Table 2. Bands that capture more extremums and inflections of $R_{rs}(\lambda)$.

Wavelength	From $f_\sigma(\lambda)$	From $f_\varsigma(\lambda)$	Proposed Bands	H&S Bands*	MODIS	MERIS
385		x	1	384		
395	x		2			
400		x		413	412	412
425		x	3			
440	x		4	435	443	443
445		x				
460		x	5	464		
475		x	6			
490	x		7	490	488	490
510		x	8			510
515	x					
520		x		532	531	
545		x	9			
555		x			551	
565	x		10			560
580		x	11	583		
615		x	12	623		620
635		x	13			
645		x		644		
655		x		655		
665	x		14		667	665
670		x		676		
685	x		15		678	681
710			16			709
750	For atmosphere correction			748		754
870	For atmosphere correction			870		870

From Hoepffner and Sathyendranath[16].

4. SUMMARY

In this study, based on an extensive measurements of remote-sensing reflectance of various aqua environments, the primary bands (in the ~400 – 700 nm range) that optimally capture the spectral signatures

of spectral R_{rs} are determined via first- and second-order derivatives. These bands are in general cover the operational bands of MODIS and MERIS, but provide suggestions of extra bands in order to provide more and improved results for remote sensing of oceanic and coastal waters.

ACKNOWELEDGMENT

We gratefully acknowledge support for this research by NASA Biology and Biogeochemistry Program and NRL 6.2 Project "Lidar and Hyperspectral Remote Sensing" and by the Cooperative Institute for Oceanographic Satellite Studies, which is supported by NOAA award NA03NES4400001.

REFERENCES

1. Z. P. Lee, and K. L. Carder, "Effect of spectral band numbers on the retrieval of water column and bottom properties from ocean color data," Applied Optics **41,** 2191-2201 (2002).
2. H. R. Gordon, D. K. Clark, J. W. Brown, O. B. Brown, R. H. Evans, and W. W. Broenkow, "Phytoplankton pigment concentrations in the Middle Atlantic Bight: Comparison of ship determinations and CZCS estimates," Applied Optics **22,** 20-36 (1983).
3. H. R. Gordon, and A. Morel, *Remote assessment of ocean color for interpretation of satellite visible imagery: A review* (Springer-Verlag, New York, 1983).
4. IOCCG, "Status and plans for satellite ocean-color missions: Considerations for complementary missions," J. A. Yoder, ed. (IOCCG, Halifax, Canada, 1998).
5. R. W. Austin, "Inherent spectral radiance signatures of the ocean surface," Ocean Color Analysis **SIO Ref. 7410,** (1974).
6. K. L. Carder, and R. G. Steward, "A remote-sensing reflectance model of a red tide dinoflagellate off West Florida," Limnol. Oceanogr. **30,** 286-298 (1985).
7. H. R. Gordon, O. B. Brown, R. H. Evans, J. W. Brown, R. C. Smith, K. S. Baker, and D. K. Clark, "A semianalytic radiance model of ocean color," J. Geophys. Res. **93,** 10,909-910,924 (1988).
8. A. Morel, "Optical modeling of the upper ocean in relation to its biogenous matter content (Case I waters)," J. Geophys. Res. **93,** 10749-10768 (1988).
9. Z. P. Lee, K. L. Carder, and K. P. Du, "Effects of molecular and particle scatterings on model parameters for remote-sensing reflectance," Applied Optics **43,** 4957-4964 (2004).
10. J. R. V. Zaneveld, "A theoretical derivation of the dependence of the remotely sensed reflectance of the ocean on the inherent optical properties," J. Geophys. Res. **100,** 13135-13142 (1995).
11. H. Loisel, and A. Morel, "Light scattering and chlorophyll concentration in Case 1 waters: A reexamination," Limnol. Oceanogr. **43,** 847-858 (1998).
12. D. Stramski, A. Bricaud, and A. Morel, "Modeling the inherent optical properties of the ocean based on the detailed composition of the planktonic community," Applied Optics **40,** 2929-2945 (2001).
13. J. T. O. Kirk, *Light & Photosynthesis in Aquatic Ecosystems* (University Press, Cambridge, 1994).
14. C. D. Mobley, *Light and Water: radiative transfer in natural waters* (Academic Press, New York, 1994).
15. S. Sathyendranath, F. E. Hoge, T. Platt, and R. N. Swift, "Detection of phytoplankton pigments from ocean color: Improved algorithms," Applied Optics **33,** 1081-1089 (1994).
16. N. Hoepffner, and S. Sathyendranath, "Effect of pigment composition on absorption properties of phytoplankton," Mar. Ecol. Prog. Ser. **73,** 11-23 (1991).
17. J. F. R. Gower, R. Doerffer, and G. A. Borstad, "Interpretation of the 685 nm peak in water-leaving radiance spectra in terms of fluorescence, absorption and scattering, and its observation by MERIS," Int. J. Remote Sensing **20,** 1771-1786 (1999).
18. A. G. Dekker, R. J. Vos, and S. W. M. Peters, "Analytical algorithms for lake water TSM estimation for retrospective analyses of TM and SPOT sensor data," Int. J. Remote Sensing **23,** 15-35 (2002).
19. IOCCG, "Remote Sensing of Inherent Optical Properties: Fundamentals, Tests of Algorithms, and Applications," in *Reports of the International Ocean-Colour Coordinating Group, No. 5*, Z.-P. Lee, ed. (2006), p. 135.

PROCEEDINGS OF SPIE

Coastal Ocean Remote Sensing

Robert J. Frouin
ZhongPing Lee
Editors

26–27 August 2007
San Diego, California, USA

Volume 6680

SPIE